



**Providing Choice & Value**  
Generic CT and MRI Contrast Agents

**FRESENIUS  
KABI**

CONTACT REP

**AJNR**

## **Hyperpolarized MR Imaging: Neurologic Applications of Hyperpolarized Metabolism**

B.D. Ross, P. Bhattacharya, S. Wagner, T. Tran and N. Sailasuta

*AJNR Am J Neuroradiol* 2010, 31 (1) 24-33

doi: <https://doi.org/10.3174/ajnr.A1790>

<http://www.ajnr.org/content/31/1/24>

This information is current as of July 21, 2025.

B.D. Ross  
P. Bhattacharya  
S. Wagner  
T. Tran  
N. Sailasuta



# Hyperpolarized MR Imaging: Neurologic Applications of Hyperpolarized Metabolism

**SUMMARY:** Hyperpolarization is the general term for a method of enhancing the spin-polarization difference of populations of nuclei in a magnetic field. No less than 5 distinct techniques (dynamic nuclear polarization [DNP]; parahydrogen-induced polarization—parahydrogen and synthesis allow dramatically enhanced nuclear alignment [PHIP-PASADENA]; xenon/helium polarization transfer; Brute Force;  $^1\text{H}$  hyperpolarized water) are currently under exhaustive investigation as means of amplifying the intrinsically (a few parts per million) weak signal intensity used in conventional MR neuroimaging and spectroscopy. HD-MR imaging in vivo is a metabolic imaging tool causing much of the interest in HD-MR imaging. The most successful to date has been DNP, in which carbon-13 ( $^{13}\text{C}$ ) pyruvic acid has shown many. PHIP-PASADENA with  $^{13}\text{C}$  succinate has shown HD-MR metabolism in vivo in tumor-bearing mice of several types, entering the Krebs—tricarboxylic acid cycle for ultrafast detection with  $^{13}\text{C}$  MR imaging, MR spectroscopy, and chemical shift imaging. We will discuss 5 promising preclinical studies:  $^{13}\text{C}$  succinate PHIP in brain tumor;  $^{13}\text{C}$  ethylpyruvate DNP and  $^{13}\text{C}$  acetate; DNP in rodent brain;  $^{13}\text{C}$  succinate PHIP versus gadolinium imaging of stroke; and  $^1\text{H}$  hyperpolarized imaging. Recent developments in clinical  $^{13}\text{C}$  neurospectroscopy encourage us to overcome the remaining barriers to clinical HD-MR imaging.

The symposium<sup>1</sup> dealt with the topic of novel contrast agents “that enhance your image.” If the definition of contrast is the addition of any new dimension, then a reasonable theme for this review—which asks whether hyperpolarized (HD)-MR imaging and spectroscopy of the brain are both feasible and contributory—would be to discuss the novel contrast that is enhanced by chemistry.

## Chemical Contrast

More than 80 brain metabolites can be distinguished and displayed (as a spectrum) by using MR spectroscopy. However, a quick glance at the metabolic diagram provided as a guide to the human single-voxel proton brain examination (the conventional and automated PROBE/SV; GE Healthcare, Milwaukee, Wisconsin) shows that we do not directly observe any metabolites of the Krebs—tricarboxylic acid (TCA—the centerpiece of cerebral mitochondrial energy metabolism) cycle and do not draw any conclusions about it or several other important aspects of brain chemistry, except by inference. Under special circumstances, the TCA cycle intermediates do appear in a human brain spectrum. As an example, succinate, at an estimated concentration of 25 mmol/L, appears at a chemical shift of 2.42 ppm. The concentration has been estimated on the basis of the reference creatine (Cr) peak at 3.02 ppm, which is generally present at a 10-mmol/L concentration (an “amount” of succinate, for the 8-cm<sup>3</sup> result, equivalent to 200  $\mu\text{mol}$ ). For future reference, for the proton spectrum, 4 min-

utes’ accumulation detected 200  $\mu\text{mol}$  of succinate, approximately 50  $\mu\text{mol}/\text{min}$ .

## Spatial Contrast

Chemical shift imaging, so-called because multiple spectra are acquired during a single MR spectroscopy examination, provides a regionally specific diagnosis of brain tumor, based on a 20% increase or more in biomarkers choline/Cr and myo-inositol/Cr ratios. However, when these individual spectral peaks are used to develop a true image from each brain metabolite, chemical shift imaging is not comparable with MR images; more often than not, a color image of the tumor marker choline is completely unreliable for diagnostic purposes.

## Exogenous Contrast

Intravenous or oral administration of exogenous chemical contrast agents, including the stable isotope carbon 13 ( $^{13}\text{C}$ ), has played a prominent part in the development of MR neurochemical diagnosis. The appearance in the brain of 1- $^{13}\text{C}$  enriched glucose, a neuronal substrate, and its conversion via the TCA cycle in real-time to neuronal  $^{13}\text{C}$  glutamate, aspartate, and other metabolites (Fig 1, right) in enriched brain spectra acquired with time, provides the metabolic flux rate of the TCA cycle, not available through  $^1\text{H}$ -MR spectroscopy or indeed from any current brain imaging method.

## “Smart” (Glial) Contrast

Distinguishing cell types is another source of contrast: In the brain, where acetate is a fuel for glia but not for neurons, 1- $^{13}\text{C}$  acetate provides in vivo images of the glial-TCA cycle rate (Fig 1, left). The  $^{13}\text{C}$  contrast in turn allows in vivo MR imaging of the glutamate-neurotransmitter flux rate, a process that involves cycling of glutamate between neurons and glia.<sup>2</sup> Recent technical advances have liberated the spectroscopist, previously confined to performing  $^{13}\text{C}$  MR spectroscopy with proton decoupling in the posterior brain, to imaging frontal brain regions believed to be responsible for most cognitive functions. Using a technique of low-power noise decoupling<sup>3</sup>, glial TCA flux can now be determined for the frontal brain (Fig 2, right). By the simple device of infusing another “smart”  $^{13}\text{C}$

From the Huntington Medical Research Institutes, Pasadena, California; and Rudi Schulte Research Institute, Santa Barbara, California.

This work was supported by the Rudi Schulte Research Institute; National Institutes of Health (National Cancer Institute: grants R01 CA 122513, 1R21 CA118509, 1K99CA134749-01); and Tobacco-Related Disease Research Program (grants 16KT-0044 and 16RT-0184).

Paper previously presented at: Annual Meeting of the American Society of Neuroradiology, May 16–21, 2009; Vancouver, British Columbia, Canada.

Please address correspondence to Brian D. Ross, MD, 10 Pico St, Pasadena, CA 91105; e-mail: Bdross.hmri@gmail.com



Indicates open access to non-subscribers at [www.ajnr.org](http://www.ajnr.org)

DOI 10.3174/ajnr.A1790

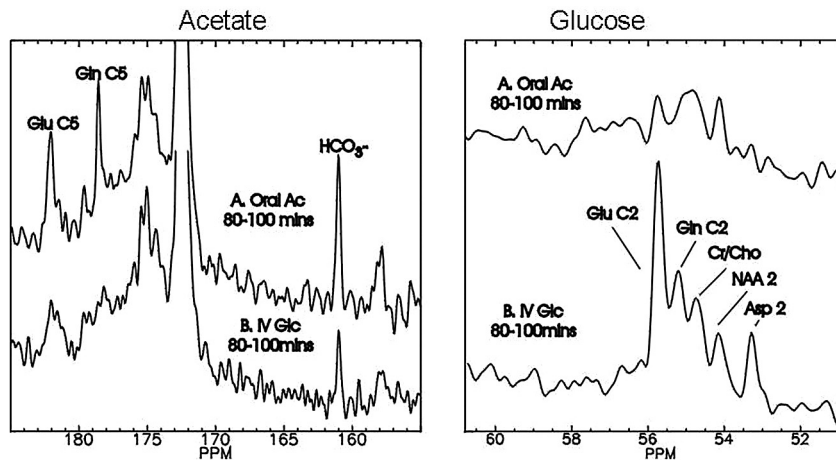
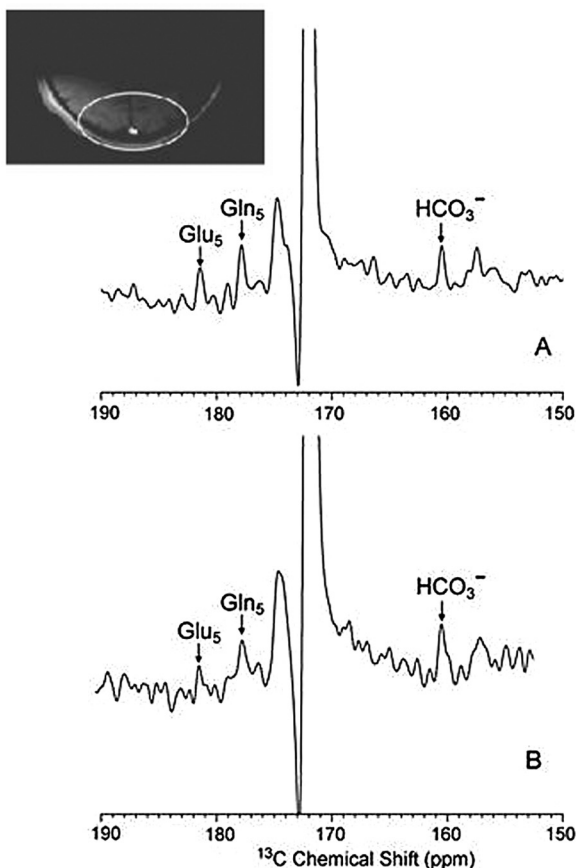
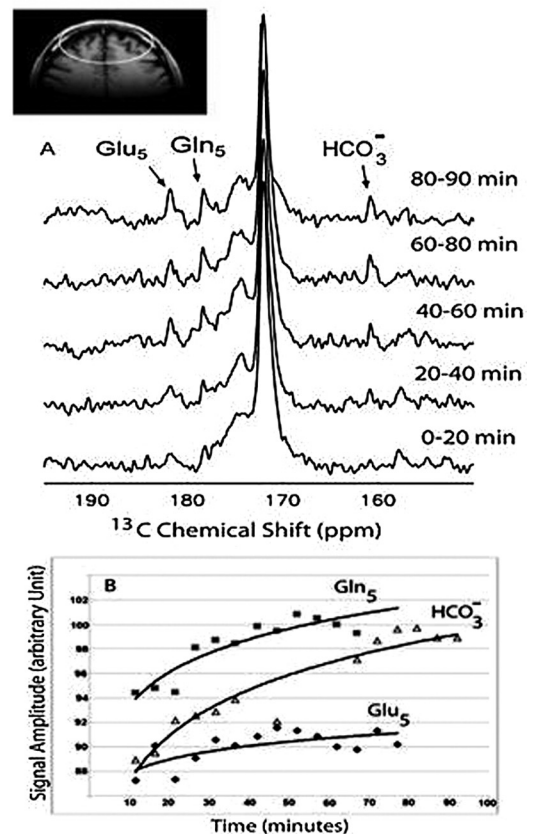


**Fig 1.** Enhanced neuronal contrast through selective  $^{13}\text{C}$  enrichment. With noninvasive  $^{13}\text{C}$  MR spectroscopy, it is possible to separately evaluate glial metabolism by use of the precursor  $1\text{-}^{13}\text{C}$  acetate (left panel), which is selectively transported into astrocytes and metabolized to glutamate (Glu) and glutamine (Gln) enriched in carbon 5 (C5). Neuronal metabolism favors  $^{13}\text{C}$  glucose (Glc, right panel), which is also converted to glutamate and glutamine, enriched in carbon 2 (C2), as well as carbons 3 and 4 (C4) (not shown). Both acetate and glucose are metabolized to  $^{13}\text{C}$  bicarbonate ( $\text{HCO}_3^-$ , left panel), respectively quantifying glial and neuronal tricarboxylic acid (TCA) cycle rates of the intact human brain. Oral Ac indicates administered load of  $1\text{-}^{13}\text{C}$  enriched sodium acetate, followed 80–100 min later by enrichment of cerebral metabolites as indicated; mins, minutes; Gln, glutamine; Asp, aspartate; Cr, creatine; Cho, choline; NAA, *N*-acetylaspartate.



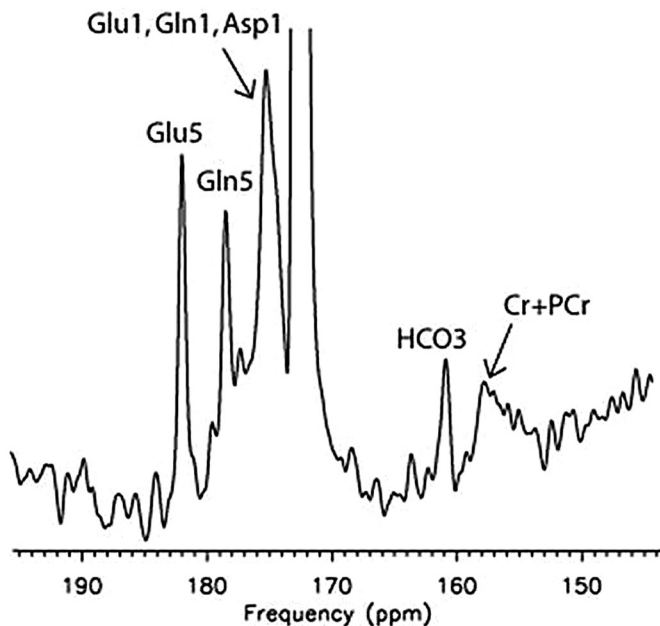
*Comparison of NOE + DC (A) and low power NOE (B) of the posterior parietal human brain in an  $[1\text{-}^{13}\text{C}]$  glucose infusion protocol.*



Enrichment of  $^{13}\text{C}$  in glutamate and glutamine in the anterior brain during  $[1\text{-}^{13}\text{C}]$  acetate infusion.

**Fig 2.** Moving to the frontal lobe through low-power  $^{13}\text{C}$  MR spectroscopy. Traditionally, in vivo  $^{13}\text{C}$  MR spectroscopy of the human brain has been confined to “safe” areas, such as the occipital cortex (left panel), to avoid heat deposition in the ocular lens. With increased interest in metabolic abnormalities of the frontal lobe involved in executive functions, a novel  $^{13}\text{C}$  MR spectroscopy method uses low-power nuclear Overhauser effect (NOE) to safely obtain glial metabolic data (right panel) from the frontal cortex. DC indicates (proton) decoupling. Reprinted with permission from *Journal of Magnetic Resonance*.<sup>3</sup> Copyright 2008, Elsevier Ltd.

## C2-glucose in Human “hind-brain”



## C2-glucose in Human “fore-brain”

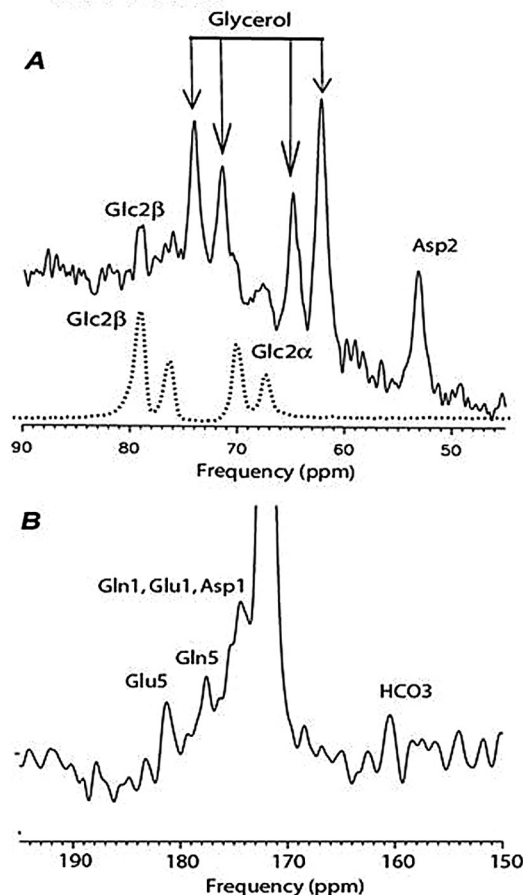


**Fig 3.**  $^{13}\text{C}$  MR spectroscopy of neuronal function in the frontal brain. To obtain equivalent data concerning neuronal function, the isotope infused must be C2-enriched  $^{13}\text{C}$  glucose which, in contrast to carbon 1 (C1)-glucose, enriches glutamate and glutamine in C5 and C1 (left panel). These products can safely be measured with a low-power NOE method in the frontal lobes (right panel). PCr indicates phosphocreatine. Reproduced with permission from *Radiology*.<sup>4</sup> Copyright 2009, Radiological Society of North America.

contrast agent, 2- $^{13}\text{C}$  glucose, rather than the convention described above, which uses 1- $^{13}\text{C}$  glucose, the  $^{13}\text{C}$  label preferentially enters carbon 5 of glutamate and glutamine. This permits neuronal (as well as glial) TCA fluxes to be imaged independently in the frontal lobe without the need for proton decoupling (Fig 3).<sup>4</sup>

### Imaging the 2-Hit Hypothesis of Clinical Glutamate Neurotransmitter Dysfunction

This level of sophistication in metabolic brain imaging invites novel hypotheses to explain the much-debated function and dysfunction of glutamate neurotransmission. Sailasuta et al<sup>5</sup> have recently proposed, in drug-abuse subjects, a 2-hit neurochemical mechanism, involving first a drastic reduction in the TCA cycle rate of frontal brain glia (Fig 4).<sup>6</sup> These patients also demonstrate significantly elevated steady-state concentrations of brain glutamate,<sup>7</sup> which in turn was hypothesized to provide the second hit, excitotoxicity of the surrounding neurons. The  $^{13}\text{C}$  MR imaging contrast will assist in establishing not only the cellular specificity but the chronology of these events to illuminate novel mechanisms for several different disorders believed to depend on altered glutamatergic neurotransmission: methamphetamine abuse, depression, multiple sclerosis,

schizophrenia, hepatic encephalopathy, epilepsy, and human immunodeficiency virus—encephalopathy.<sup>8</sup>

### Temporal Contrast

In the esoteric world of neurotransmitter chemistry, yet another compartment, the extracellular or synaptic space, becomes important as well as the element of time. With the duration of a typical action potential equivalent to 50 ms and a common epileptic seizure equivalent to <1 minute, rapid changes in extracellular glutamate and glutamine can be defined and the predicted changes in intracellular glutamate and glutamine can be detected with either  $^{13}\text{C}$  or nitrogen 15 ( $^{15}\text{N}$ ) MR spectroscopy in vivo (Kanamori, unpublished work in the laboratory, 2009). Neuroimaging techniques would ideally be completed in a similar time scale. Although that is currently feasible for x-ray, CT, electroencephalography, and magnetoencephalography, none of these imaging techniques command the necessary chemical contrast; conventional positron-emission tomography (PET) and MR spectroscopy each require several minutes to form an in vivo image. The  $^{13}\text{C}$  MR spectroscopy studies described above typically occupy  $\geq 1$  hour.



# Two-Hit Hypothesis of Drug Abuse

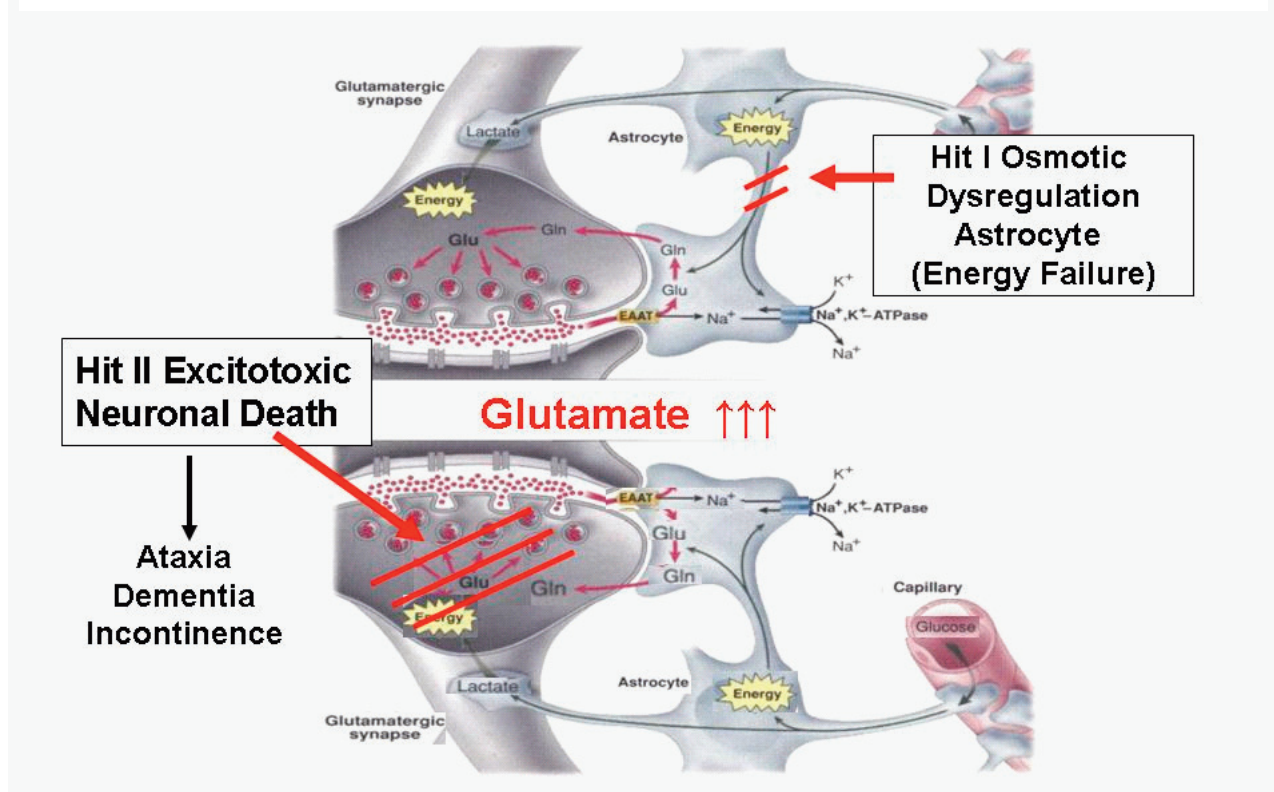


**Fig 4.**  $^{13}\text{C}$  MR spectroscopy schematic for examining the “two-hit” hypothesis of drug abuse in the frontal brain. Combining dynamic  $^{13}\text{C}$  measures of glial and neuronal glutamate metabolism with  $^1\text{H}$ -MR spectroscopy assays of steady-state glutamate concentration provides a novel window on drug abuse. Inhibition of acetate metabolism by methamphetamine (Meth) abuse indicates a possible mechanism whereby reduced clearance of glutamate in glia (hit 1) results in glutamate excitotoxicity of neurons (hit 2). Variations on this theme may contribute to other neurologic syndromes for which selective assays of glial and neuronal function provide enhanced imaging tools. Na indicates sodium; ATPase, adenosine triphosphatase; K, potassium; EAAT, excitatory amino acid transporter. Reprinted with permission from *Science*.<sup>6</sup> Copyright 1999, The American Association for the Advancement of Science.

## Need for HD-MR Imaging

The need for a new imaging technique in neuroradiology is clear from the preceding arguments. Water-based MR imaging, which can be completed in seconds, has diversified as each new spin property of protons is exploited. The problem for chemical contrast is the inherently low metabolite concentrations, all of which lie between 0.1 and 10.0 mmol/L, a level some 8000–100,000-fold lower than that of the protons in water (80 mol/L). HD-MR imaging offers a means of closing the gap. Conventional (Boltzmann) MR imaging depends on the population of nuclear spins, which can be brought to a different energy state in a static magnetic field, generally a few parts per million. Raising the population of nuclei at this higher energy level to unity would enhance MR signal intensity approximately 250,000-fold, not simply a few-fold as is obtained by moving to high-field 3T, 7T, or 9.4T MR imaging scanners but up to the needed level for parity with proton MR imaging, which as we pointed out, is 8,000–100,000-fold.

Methods for HD-MR imaging have proliferated<sup>9–15</sup> since the first parahydrogen-induced polarization (PHIP) was explored 20 years ago. Five methods are illustrated by the equip-

ment acquired to prepare the exogenous contrast agent for each one (Fig 5). In Fig 5, top left, is the rather simple equipment consisting of a very-low-field magnet (red), driven by a computer and through which reagents can be pumped while mixed and heated with parahydrogen gas (the source of high-polarized nuclei) and a catalyst, norbornadiene. Hydrogenation is followed by spin transfer from the hydrogen to  $^{13}\text{C}$ , in which high polarization can be retained for several tens of seconds. This contrast agent now needs to be injected rapidly into a biologic system, held within a conventional MR spectrometer.

The lower left of Fig 5 illustrates a commercial dynamic nuclear polarization (DNP) device (Hypersense; Oxford Instruments Molecular Biotools, Witney, UK). Here, the principle is quite different and involves no chemical synthesis. The  $^{13}\text{C}$  reagent is exposed, at very low temperature and high field, to irradiation, whereby the almost complete polarization of unpaired electrons is transferred to nuclei (“dynamic nuclear polarization”). The only exogenous agent apart from the  $^{13}\text{C}$ -enriched substrate is a free radical, which ideally would be removed before injection. Most familiar of hyperpolarization technologies, optical pumping (Fig 5, top right) has, for many

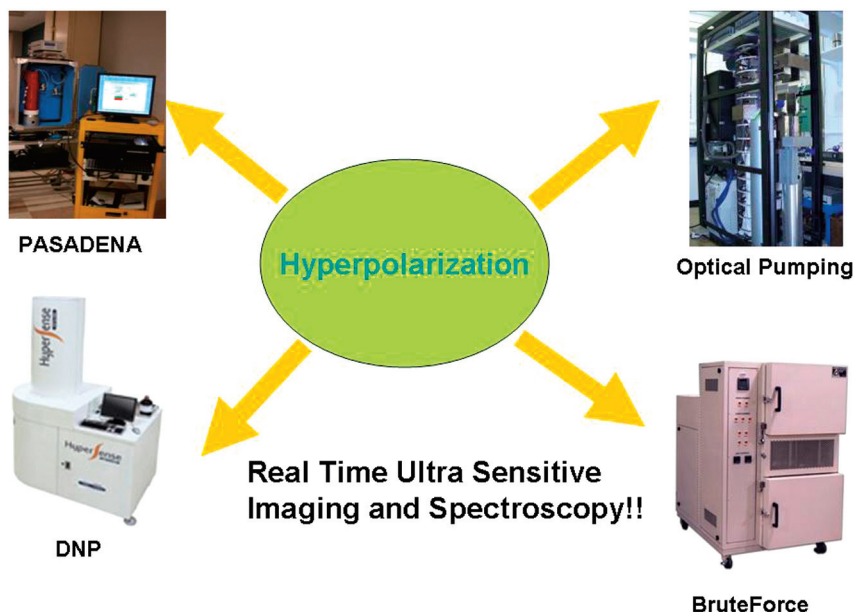


**Fig 5.** Four methods for hyperpolarized-MR imaging and spectroscopy. In the historic order of discovery, parahydrogen-induced polarization (PASADENA); optical pumping of noble gases helium and xenon; dynamic nuclear polarization (DNP); and Brute Force have each been harnessed to the challenge of increasing enhancement above the Boltzmann distribution of approximately 1 ppm toward unity, with upwards of 10,000-fold enhancement of MR signal intensity for in vivo MR imaging and MR spectroscopy.

years, permitted human lung imaging after inhalation of the hyperpolarized noble gases helium or xenon. Most recently Lisitza et al<sup>16</sup> demonstrated the transfer of polarization from the gas to a  $^{13}\text{C}$  molecule of interest. Expansion of the methodology and improvements beyond the 3- to 20-fold signal-intensity enhancement for  $^{13}\text{C}$  so far achieved will make this a valuable method because no catalyst or other addition is required and the gas phase, which is volatile, can easily be removed before injection.

Figure 5 bottom right illustrates another device that uses low field and low temperature alone (BruteForce, Millikelvin Technologies, Marblehead, Massachusetts) to hyperpolarize any  $^{13}\text{C}$ -enriched compound. While kept at a low temperature, the hyperpolarized  $^{13}\text{C}$  reagent, to which there have been no chemical additions, can be shipped over distances. Finally, and not illustrated, is the technique of hyperpolarization of water,<sup>17</sup> which on injection into an animal, enhances the MR image 2–3-fold above the enhancement of the native water. While the image enhancement so far achieved is relatively small, the potential of using water as a natural contrast agent is obvious.

### HD-MR Imaging in Practice

First published under the smart acronym PASADENA (parahydrogen and synthesis allow dramatically enhanced nuclear alignment) but synchronously and subsequently known as PHIP in 1987,<sup>18</sup> it took 24 years from invention to bioimaging. With a highly toxic  $^{13}\text{C}$ -enriched contrast agent and acetone as the required solvent, not surprisingly this subsecond  $^{13}\text{C}$  PHIP imaging, while technically “in vivo,” was lethal.<sup>19</sup> The first water-soluble reagent capable of PHIP was hydroxymethyl acrylate, which on (para)-hydrogenation becomes  $^{13}\text{C}$  hydroxyethylpropionate (HEP), developed by Amersham (Malmo, Sweden) and used in surviving animals to provide ultrafast  $^{13}\text{C}$  angiography in pigs.<sup>20</sup> HEP is toxic, as is the novel catalyst, but 2 successor molecules developed at Huntington Medical Re-

search Institutes, Pasadena, California, 1- $^{13}\text{C}$  malic acid<sup>10</sup> (Fig 6, left) and 1- $^{13}\text{C}$  fumaric acid<sup>14</sup> (Fig 6, right), both provided a practical synthetic route to the biologic intermediate of the Krebs-TCA cycle, 1- $^{13}\text{C}$  succinate. Also illustrated in Fig 6 are the chemical process, the molecular addition of parahydrogen under the influence of a specific catalyst and the spin physics of polarization transfer,<sup>21</sup> which were developed in Malmo, Sweden, to dramatically elevate the yield and bring hyperpolarization to  $\geq 40\%$  within a few seconds in the specially designed polarizer. Quality assurance routines achieved somewhat lower but still impressive levels of hyperpolarization of 1- $^{13}\text{C}$  succinate to the high degree of reproducibility suited to biologic experimentation (Fig 7).<sup>22,23</sup>

### HD-MR Imaging of the Brain

The earliest known attempt to image the brain with HD-MR imaging used PHIP with HEP (Fig 8),<sup>24</sup> a reagent which, in the time scale of the study, did not pass beyond the vasculature and, as far as is known, cannot be metabolized further. Ultrafast  $^{13}\text{C}$  angiography may, nevertheless, be of value, as shown previously<sup>19</sup> for the coronary vasculature, because there is no background signal intensity. The first intracerebral  $^{13}\text{C}$  HD-MR imaging attempted used a novel  $^{13}\text{C}$  reagent, 1- $^{13}\text{C}$  maleate plus succinate<sup>10</sup> (not shown here), in tumor-bearing rats. While the reagent appeared to enter the brain, crossing the blood-brain barrier (BBB), no cerebral metabolites were identified. A biopsy examined later when the brain was at a Boltzmann state did, however, indicate that succinate had entered the tumor (Fig 9) and had been further metabolized to bicarbonate, glutamine, and glutamate. The biopsy findings of normal host brain tissue were devoid of  $^{13}\text{C}$  succinate and its metabolites, suggesting that PHIP of succinate might in the future provide a specific contrast agent for cerebral tumor in vivo. Due to the need for a unique glial substrate in  $^{13}\text{C}$  neurospectroscopy (see above), 1- $^{13}\text{C}$  acetate was hyperpolarized by DNP and shown to enter the head during a

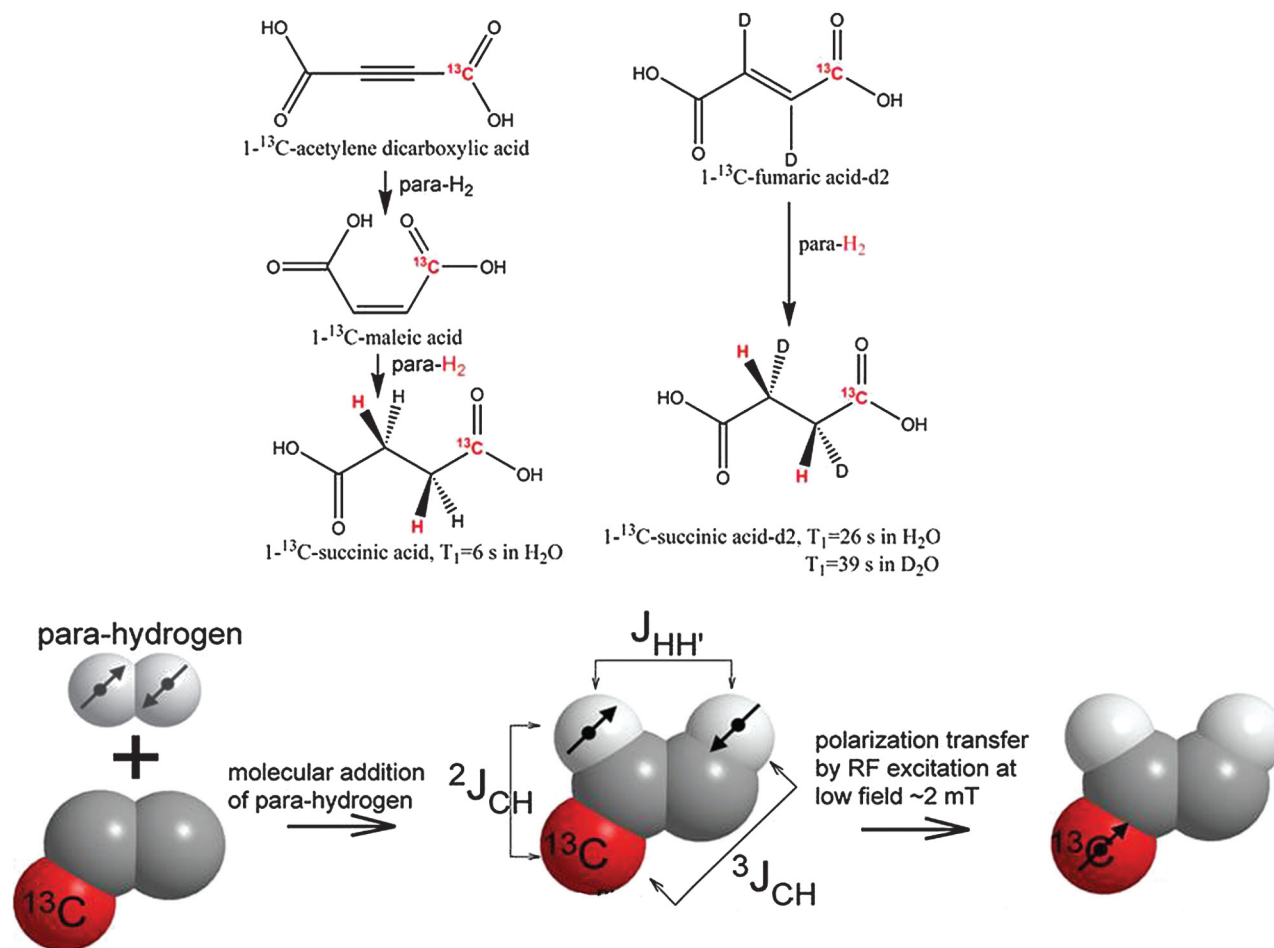
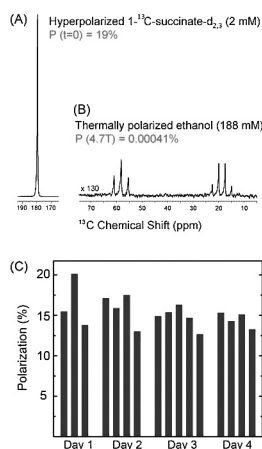


**Fig 6.** Two techniques for producing hyperpolarized  $^{13}\text{C}$  succinate, the first biologic imaging agent generated by the parahydrogen method. Starting with the toxic precursor acetylene dicarboxylic acid (left panel) or with the biologically safe  $1-^{13}\text{C}$  fumarate (right panel), a high degree of polarization can be achieved during the molecular addition of parahydrogen, followed by polarization transfer to the  $^{13}\text{C}$  atom shown in red (below). D indicates deuterium;  $\text{d}_2$ , deuteration; RF, radio-frequency; mT, milli-Tesla; HO, hydroxyl; H, hydrogen; T, spin relaxation time (seconds);  $\text{D}_2\text{O}$ , deuterized water;  $^1\text{HH}$ , proton-carbon coupling constants;  $^2\text{CH}$ , carbon-carbon coupling constants.



$^{13}\text{C}$  spectra of hyperpolarized 1.95 mM  $1-^{13}\text{C}$ -succinate- $\text{d}_{2,3}$  using HMRI-laminar flow clinical prototype polarizer (A) and thermally polarized ethanol (B) (188 mM  $^{13}\text{C}$  per each carbon site) acquired at 4.7 T. =47,000. (C) Hyperpolarization chart of  $1-^{13}\text{C}$ -succinate- $\text{d}_{2,3}$  of 16 experiments to determine the reproducibility of the polarizer. =15.3 $\pm$ 1.9%.

**Fig 7.** Quality assurance and reproducibility of hyperpolarization. A–C, The signal-intensity enhancement (19% polarization equivalent to 47,000-fold) due to hyperpolarization, estimated by comparison of the test reagent (A) with a standard solution of natural-abundance  $^{13}\text{C}$  ethanol (B), while remarkably constant during 4 days and 16 successive in vitro experiments (C), is more variable in vivo. The effects of dilution, mixing in blood, circulation times,  $T_1$  relaxation time of the  $^{13}\text{C}$  (and  $^{15}\text{N}$ ) reagents, combined with the effects of radio-frequency pulses used for signal-intensity detection significantly reduce available signal-intensity enhancement in vivo. HMRI indicates Huntington Medical Research Institutes; P = polarization (%).

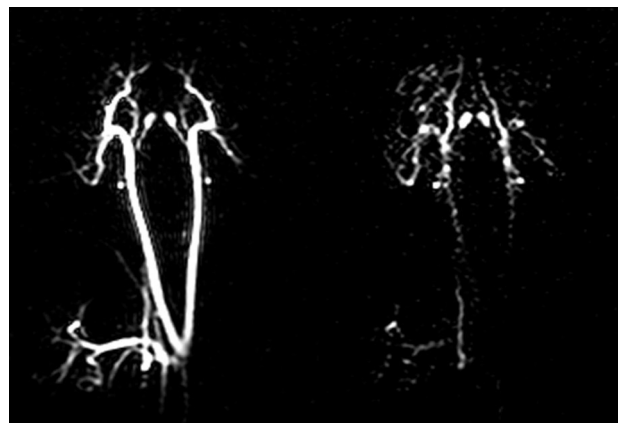


**Fig 8.** Real-time  $^{13}\text{C}$  PASADENA images of carotid artery and major blood vessels of the pig brain. Two of a time-lapse series of images obtained subsequent to a single injection of aqueous hydroxyethyl propionate ( $1-^{13}\text{C}$ ) with initial polarization  $P = 0.4$ .

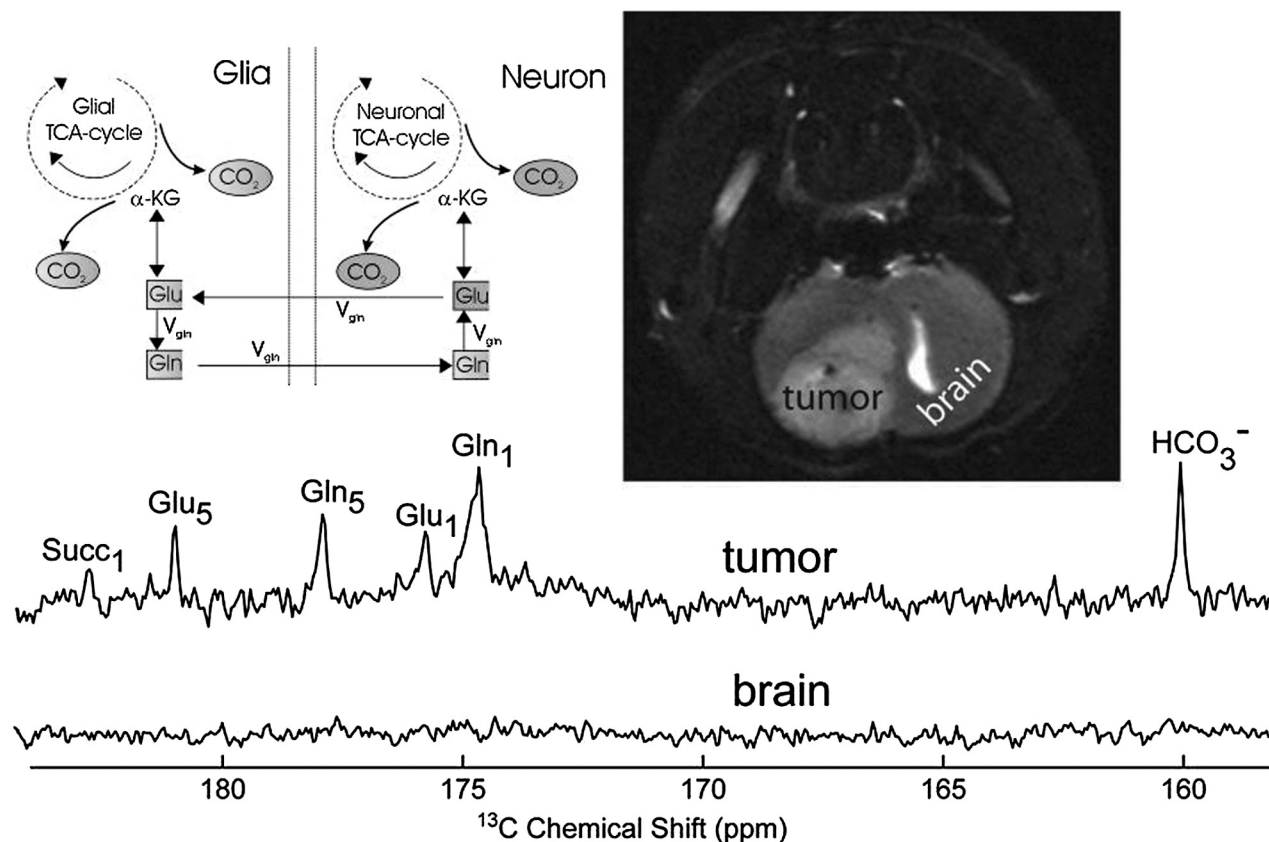


**Fig 9.** Toward hyperpolarized  $^{13}\text{C}$  succinate imaging of brain cancer. In this early study,  $^{13}\text{C}$  hyperpolarized images of the 9L brain tumor are obtained, but no metabolites are detected in vivo when hyperpolarized "succinate" (generated from  $^{13}\text{C}$  acetylene dicarboxylic acid; Fig 6, left) is injected via the jugular vein. Harvested brain tumor subsequently showed nonhyperpolarized  $^{13}\text{C}$  metabolites anticipated from metabolism of  $^{13}\text{C}$  succinate (Succ) through the neuronal and glial pathways indicated. No metabolites were isolated from the intact brain, indicating possibly the importance of a defective blood-brain barrier (BBB) for in vivo hyperpolarization neuroimaging.  $\alpha$ -KG indicates alpha-ketoglutarate;  $V_{gh}$ , velocity glutamine-glutamate cycle. Reprinted with permission from *Journal of Magnetic Resonance*.<sup>10</sup> Copyright 2007, Elsevier Ltd.

2-minute imaging session.<sup>13</sup> As with the preceding PHIP study, the intact BBB may have delayed entry into the brain, which was not categorically enhanced in this HD-MR imaging of 1- $^{13}\text{C}$  acetate.

The critical problem of BBB may be circumvented by testing  $^{13}\text{C}$ -PHIP reagents in animals with extracerebral tumors.<sup>25</sup> Prolonged imaging times can be obtained by using PHIP to hyperpolarize  $^{15}\text{N}$  incorporated in the tumor biomarker choline, which is then detected by using ultrafast  $^{15}\text{N}$  MR spectroscopy in vivo.<sup>26</sup>

The first success in ultrafast  $^{13}\text{C}$  brain imaging was described by R. Hurd and colleagues at the University of California, San Francisco (personal communication, 2009), using DNP to hyperpolarize the pyruvate analog ethyl 1- $^{13}\text{C}$ -pyruvate (E-P). Not only was hyperpolarized E-P identified in the intact rat brain after intravenous injection, but several of its anticipated neurometabolites were visualized in  $^{13}\text{C}$  spectra and images. E-P has a long history as a safe antishock and neuroprotective agent in animals and in man<sup>27</sup>; therefore, it appears poised to be the first clinical HD-MR neuroimaging reagent.

A parallel study with PHIP 1- $^{13}\text{C}$  succinate recently confirmed that, once the BBB has been disrupted, in this case by experimental stroke (Fig 10), this HD-MR imaging technology can also achieve ultrafast neuroimaging. Most interesting,  $^{13}\text{C}$  succinate chemical shift is pH-sensitive over a wide range

(Fig 11). Two hyperpolarized  $^{13}\text{C}$  resonances within the brain of a rat manifesting stroke (Fig 11, inset) may represent unmetabolized  $^{13}\text{C}$  succinate at an acid pH and a reduced metabolic product,  $^{13}\text{C}$  malate, within the stroke.<sup>28</sup> The latter may reflect the altered mitochondrial redox state expected in stroke brain.<sup>29</sup> If confirmed, one could imagine an extension of current emergency stroke MR imaging protocol to include a sub-second assay of tissue pH and redox state by using HD-MR imaging, because this may be more predictive of tissue viability than an assay of lactate or diffusion-weighted imaging alone.

### Roll Over Warburg and Tell Hans Krebs the News!

Given the not inconsiderable technical challenge of bringing HD-MR imaging to the neuroradiology clinic, what "killer application" can we envisage on the basis of these early and faltering steps? Glioblastoma multiforme expresses the oncoprotein hypoxia-induced factor (HIF)-1 $\alpha$  at an exceptionally high titer (Fig 12). In examining a representative extracerebral tumor renal cancer (RENCA) cell, believed to express succinate dehydrogenase oncogene, almost the entire Krebs-TCA cycle was successfully imaged by using the PHIP reagent hyperpolarized 1- $^{13}\text{C}$  succinate (Fig 13), while another tumor, lymphoma A-20 expressing HIF-1 $\alpha$ , albeit at a much lower titer than that of glioblastoma, metabolized 1- $^{13}\text{C}$  succinate through the TCA cycle only as far as malate.<sup>25</sup> If tumors do



## Succinate Enters "Stroke" Brain

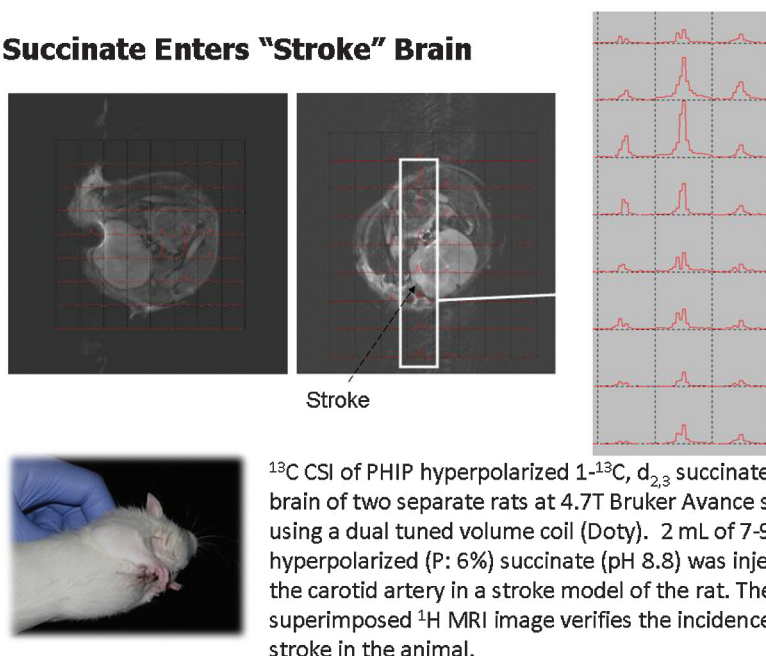


**Fig 10.** In vivo neuroimaging and spectroscopy of hyperpolarized <sup>13</sup>C succinate. In confirmation of the role of BBB, the first truly in vivo hyperpolarized <sup>13</sup>C spectra arose predominantly from the stroke region of rat brain (left and center) as shown in 2D ultrafast chemical shift imaging (CSI) series (right panel) (Avance, Bruker, Karlsruhe, Germany). PHIP indicates parahydrogen-induced polarization.

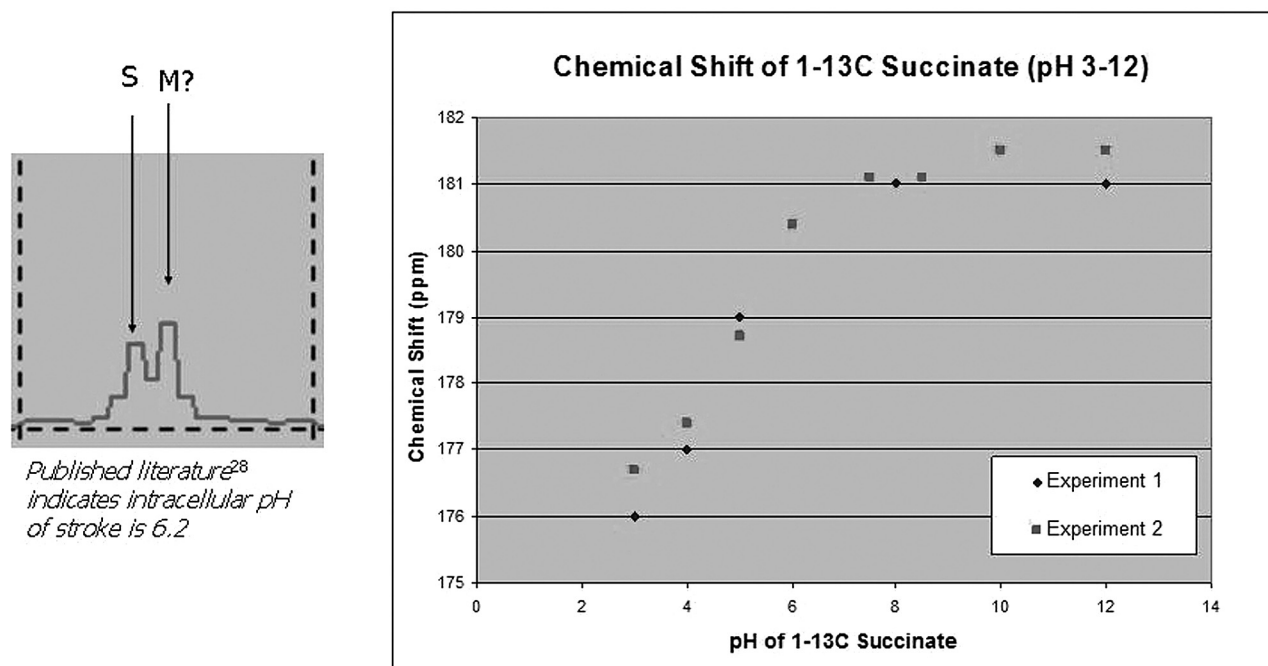


**Fig 11.** Hyperpolarized <sup>13</sup>C metabolites of succinate in stroke brain. The effect of in vitro pH was verified on chemical shift of <sup>13</sup>C succinate (right). A spectrum (inset) from the in vivo hyperpolarized dataset in Fig 10 indicates 2 resonances that are tentatively assigned to <sup>13</sup>C succinate (S) at approximately pH 8 and its hyperpolarized metabolic product, C4 malate (M). The intracellular pH of stroke in vivo might, in the future, be estimated from hyperpolarized <sup>13</sup>C spectra acquired in 3.5 seconds. Suc indicates succinate. (T. Tran and N. Sailasuta, unpublished data, HMRI, May 2009)

indeed have functional TCA, we must first question the Warburg hypothesis of cancer biochemistry, perhaps replacing it with the Krebs-TCA hypothesis. Perhaps HD-MR imaging can fill the gap left by 2-deoxyglucose PET in brain scans performed for early diagnosis and therapeutic monitoring of metabolically more active tumors, such as glioblastoma.

## Summary and Conclusions

First, HD-MR imaging, of which there are no less than 5 competing technologies, has been successful in 2 preclinical demonstrations of neuroimaging and spectroscopy. DNP of E-P may offer imaging and neuroprotection after shock and brain injury.<sup>27</sup> PHIP may offer an early and specific diagnosis for

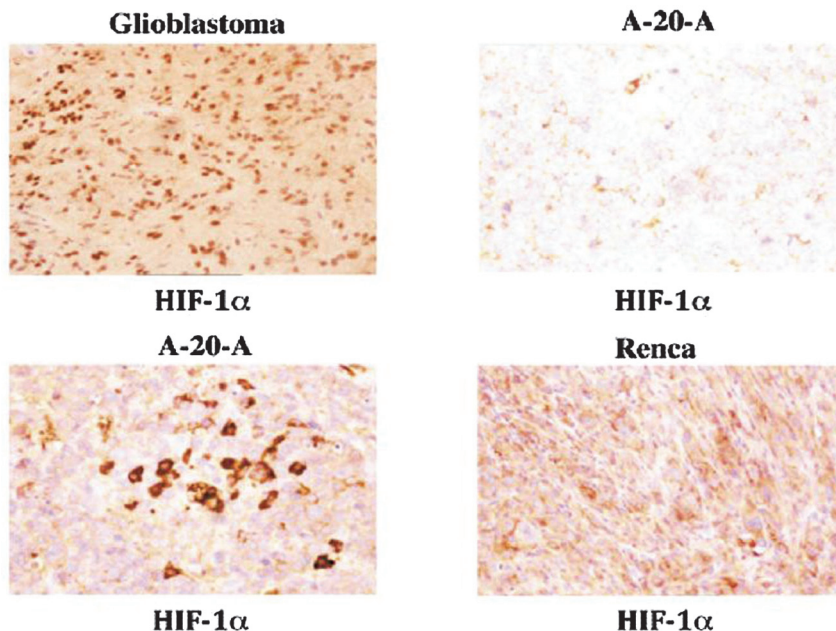


**Fig 12.** New directions for enhanced  $^{13}\text{C}$  imaging of brain cancer. Immunocytochemical stain for the hypoxia-induced factor (HIF)-1 $\alpha$  indicates glioblastoma to be particularly rich in this cancer biomarker protein. This may, in the future, provide a uniquely sensitive means of in vivo imaging of brain cancer grade and metabolic activity (see Fig 13). RENCA, renal cancer; A-20-A (top left, top right, and bottom right  $\times 160$ ; bottom left  $\times 312$ ). (Courtesy of Dr. Ashraf Imam).

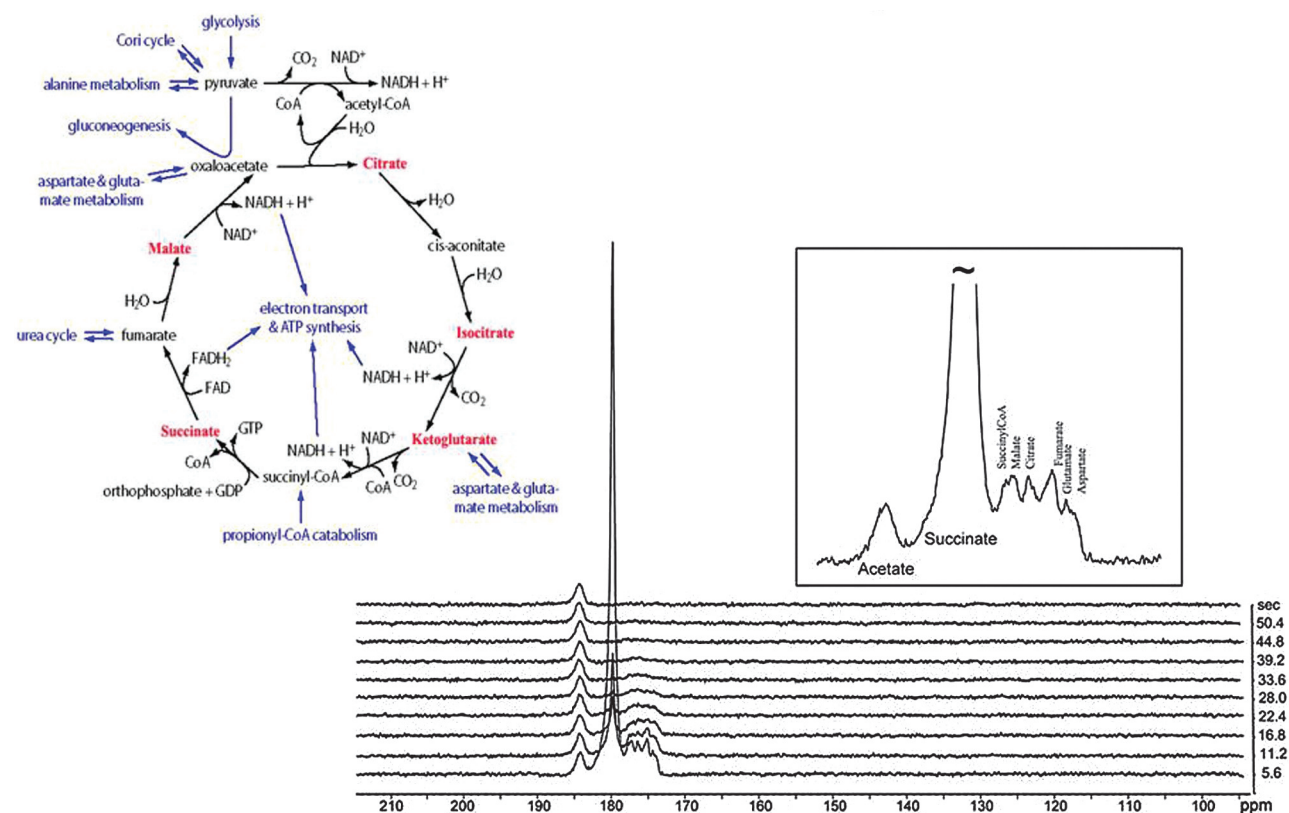


**Fig 13.** Hyperpolarized  $^{13}\text{C}$  succinate—a probe for the in vivo TCA cycle. Subcutaneous RENCA was used to demonstrate the potential for subsecond imaging of the Krebs (TCA) cycle in vivo. Not yet achieved in intact brain (see Fig 9), this novel means of enhancing metabolic images may be effective when used with short-term opening of the BBB. For abbreviations in this depiction of the Krebs tricarboxylic acid cycle, please see standard texts: metabolite peaks associated with those intermediates displayed in red were enriched in this model tumor and appear as hyperpolarized  $^{13}\text{C}$  resonances during the first 18 seconds after intravenous (IV) injection of 6 micromoles  $^{13}\text{C}$  succinate.

tumor and for stroke, based on unique  $^{13}\text{C}$  metabolic profiles obtained in seconds. Detection of HD-MR imaging of  $^{13}\text{C}$  succinate does appear to fulfill its promise of enhancing our in

vivo brain images  $\gg 10,000$ -fold. (Calculations are based on estimates of the  $^{13}\text{C}$  succinate observed by HD-MR imaging in rodent stroke of between 0.05 and 0.5  $\mu\text{mol}$  in 3 seconds [ $= 0.1$

mol/sec]. This compares with  $^1\text{H}$  succinate observed in human brain with conventional  $^1\text{H}$ -MR spectroscopy of 50  $\mu\text{mol}$  per minute. HD-MR imaging/conventional  $^1\text{H}$ -MR spectroscopy =  $60 \times 500 = 30,000$  signal enhancement.) The remaining technologies,  $^{13}\text{C}$ -xenon hyperpolarized  $\text{H}_2\text{O}$  and Brute Force, while promising, currently deliver much lower degrees of polarization (3- to 20-fold enhancements, respectively) and, to our knowledge, have not yet been attempted in the brain.

Second, no successful clinical application can be reported at this time (apart from the highly successful optical pumping of helium and xenon to generate 30,000-fold image enhancement of healthy and diseased lungs). Obstacles to DNP and PHIP are similar and will likely be overcome first for applications in oncology, cardiology, or angiography. T1, the length of time for which hyperpolarization is preserved, is characteristically  $<1$  minute and remains the Achilles heel of HD-MR imaging generally. T1 is receiving increasing attention from chemists and spin physicists and may be "solved" in a number of different ways, from use of  $^{15}\text{N}$  with intrinsically longer T1, inverse detection ("spin-storage"), or by prolonging the singlet state.<sup>30</sup>

Third, the good news for HD-MR imaging is that, despite all the difficulties in its implementation, lesser degrees of hyperpolarization can have a major impact on applications in which stable-isotope flux is diagnostic; this includes  $^{13}\text{C}$  MR spectroscopy of neuronal-glial interactions, which play an increasingly important role in understanding neurologic function and dysfunction. While it is true that 100,000-fold signal-intensity enhancement by HD-MR imaging would bring MR imaging sensitivity (currently  $10^{-3}$  Molar) into line with PET sensitivity ( $10^{-9}$  Molar), less dramatic advances have significant value. Ten- or 20-fold image enhancement would reduce conventional MR imaging times by 90%. Once implemented, clinical experience will teach us, as it has so often before, how a novel imaging technology offers new ways of thinking about the brain from which new clinical applications arise.

## Acknowledgements

We would like to thank Henry Chan, MD; Eduard Chekmenev, PhD; Kent Harris, PhD; William Perman, PhD; and Lawrence Robertson for their valuable contributions.

## References

- Barker P. **How to enhance your image.** Advanced Imaging Seminar: Contrast Agents. *Proc ASNR*; 2009, Vancouver, Canada.
- Ross B, Lin A, Harris K, et al. **Clinical experience with  $^{13}\text{C}$  MRS in vivo.** *NMR Biomed* 2003;16:358–69
- Sailasuta N, Robertson LW, Harris KC, et al. **Clinical NOE  $^{13}\text{C}$  MRS for neuropsychiatric disorders of the frontal lobe.** *J Magn Reson* 2008;195:219–25. Epub 2008 Sep 17
- Gropman AL, Sailasuta N, Harris KC, et al. **Ornithine transcarbamylase deficiency with persistent abnormality in cerebral glutamate metabolism in adults.** *Radiology* 2009;252:833–41
- Sailasuta N, Harris KC, Abulseoud O, et al.  **$^1\text{H}$ - $^{13}\text{C}$  acetate MRS to study glial glutamate dysfunction in methamphetamine users.** *Proc Int Soc Magn Reson Med* 2009;17:92
- Magistretti PJ, Pellerin L, Rothman DL, et al. **Energy on demand.** *Science* 1999;283:496–7
- Abulseoud O, Sailasuta N, Hernandez M, et al. **Impact of depression on cerebral glutamate and cognitive function in abstinent methamphetamine users.** *Proc Int Soc Magn Reson Med* 2009;17:210
- Sailasuta N, Shriner K, Ross B. **Evidence of reduced glutamate in the frontal lobe of HIV-seropositive patients.** *NMR Biomed* 2009;22:326–31
- Golman K, Ardenkjaer-Larsen JH, Petersson JS, et al. **Molecular imaging with endogenous substances.** *Proc Natl Acad Sci U S A* 2003;100:10435–39
- Bhattacharya P, Chekmenev EY, Perman WH, et al. **Towards hyperpolarized ( $^{13}\text{C}$ -succinate) imaging of brain cancer.** *J Magn Reson* 2007;186:150–55
- Bhattacharya P, Harris K, Lin AP, et al. **Ultra fast steady state free precession imaging of hyperpolarized  $^{13}\text{C}$  in vivo.** *Magnetic Resonance Materials in Physics, Biology and Medicine*; 2005;18:245–56
- Chen AP, Tropp J, Hurd RE, et al. **In vivo hyperpolarized  $^{13}\text{C}$  MR spectroscopic imaging with  $^1\text{H}$  decoupling.** *J Magn Reson* 2009;197:100–06. Epub 2008 Dec 13
- Comment A, Uffmann K, Jannin S, et al. **In vivo DNP-enhanced  $^{13}\text{C}$ -labeled acetate brain studies in a 9.4T animal scanner.** *Proc Int Soc Magn Reson Med* 2007;15:369
- Chekmenev EY, Hovener J, Norton VA, et al. **PASADENA hyperpolarization of succinic acid for MRI and NMR spectroscopy.** *J Am Chem Soc* 2008;130:4212–13. Epub 2008 Mar 12
- McCarney ER, Armstrong BD, Lingwood MD, et al. **Hyperpolarized water as an authentic magnetic resonance imaging contrast agent.** *Proc Natl Acad Sci U S A* 2007;104:1754–9
- Lisitz N, Chekmenev EY, Muradian I, et al. **Enhanced biomedical  $^{13}\text{C}$  NMR by thermal mixing with hyperpolarized  $^{129}\text{Xe}$ .** In: *Proceedings of Annual Meeting of Experimental NMR Conference*, Pacific Grove, CA. March 2–April 3, 2009
- Lingwood MD, Tokuyama ST, Brown ER, et al. **Continuous flow dynamic nuclear polarization of water under ambient conditions for in-vivo perfusion MRI.** In: *Proceedings of the 17th Scientific Meeting and Exhibition of the International Society for Magnetic Resonance in Medicine*, Honolulu. April 18–24, 2009:2456
- Bowers CR, Weitekamp DP. **Parahydrogen and synthesis allow dramatically enhanced nuclear alignment.** *J Am Chem Soc* 1987;109:5541–42
- Golman K, Axelsson O, Johannesson H, et al. **Parahydrogen-induced polarization in imaging: subsecond ( $^{13}\text{C}$ ) angiography.** *Magn Reson Med* 2001;46:1–5
- Magnusson P, Johansson E, Mansson S, et al. **Passive catheter tracking during interventional MRI using hyperpolarized  $^{13}\text{C}$ .** *Magn Reson Med* 2007;57:1140–47
- Goldman M, Johannesson H, Axelsson O, et al. **Hyperpolarization of  $^{13}\text{C}$  through order transfer from parahydrogen: a new contrast agent for MRI.** *Magn Reson Imaging* 2005;23:153–7
- Hovener JB, Chekmenev EY, Harris KC, et al. **PASADENA hyperpolarization of  $^{13}\text{C}$  biomolecules: equipment design and installation.** *MAGMA* 2009;22:111–21
- Hovener JB, Chekmenev EY, Harris KC, et al. **Quality assurance of PASADENA hyperpolarization for  $^{13}\text{C}$  biomolecules.** *MAGMA* 2009;22:123–34
- Mansson S, Johansson E, Magnusson P, et al.  **$^{13}\text{C}$  imaging—a new diagnostic platform.** *Eur Radiol* 2006;16:57–67
- Bhattacharya P, Ross B. **Imaging TCA cycle metabolism by PHIP hyperpolarization of  $^{13}\text{C}$  succinate in vivo.** *Radiology* 2009, Submitted.
- Bhattacharya P, Ross B. **Hyperpolarized  $^{15}\text{N}$  NMR: D15NP and PASADENA.** In: Lajtha A, Reith ME, eds. *Handbook of Neurochemistry and Molecular Neurobiology*. Vol 4. 3rd ed. New York: Springer; 2009
- Kim J, Young-Mi Y, Seung-Woo K, et al. **Anti-inflammatory mechanism is involved in ethyl pyruvate-mediated efficacious neuroprotection in the post-ischemic brain.** *Brain Res* 2005;1060:188–92
- Combs DJ, Dempsey RJ, Maley M, et al. **Relationship between plasma glucose, brain lactate, and intracellular pH during cerebral ischemia in gerbils.** *Stroke* 1990;21:936–42
- Shino A, Matsuda M, Handa J, et al. **Poor recovery of mitochondrial redox state in CA1 after transient forebrain ischemia in gerbils.** *Stroke* 1998;29:2421–25
- Carravetta M, Levitt MH. **Long-lived nuclear spin states in high-field solution NMR.** *J Am Chem Soc* 2004;126:6228–29